Thermal annealing of arsenic tri-sulphide thin film and its influence on device performance

Duk-Yong Choi,[a] Steve Madden, Douglas Bulla, Rongping Wang, Andrei Rode, and Barry Luther-Davies

Centre for Ultra-high Bandwidth Devices & Optical Systems (CUDOS), Laser Physics Centre, Research School of Physics and Engineering, The Australian National University, Canberra ACT 0200, Australia

(Received 9 November 2009; accepted 13 January 2010; published online 4 March 2010)

Arsenic tri-sulphide (As_2S_3) thin film waveguides have been used successfully as nonlinear optical devices for all-optical signal processors. For such devices, low propagation loss is vital if high performance is to be obtained. In this study, thermal annealing was employed not only to stabilize the physical properties of the films, but also to reduce the sources of light attenuation in the as-deposited material. Here we investigated heat-induced changes to the microstructure and optical properties of As_2S_3 thin films and, based on this information, determined the best annealing conditions. The refractive index of the films rises with annealing due to thermal densification and increased heteropolar bond density. The growth of surface roughness and thermal stress in the film, however, limits the annealing temperature to ~130 °C. We fabricated and analyzed waveguides produced from as-deposited and annealed films and found that the propagation loss of the guides dropped by ~0.2 dB/cm as a result of appropriate annealing. Rayleigh scattering and absorption from defects associated with phase separation, homopolar bonds, voids, and dangling bonds in the as-deposited film are shown to contribute to the higher light attenuation in unannealed films.
 [doi:10.1063/1.3310803]

I. INTRODUCTION

Chalcogenide glasses (ChGs) are a range of inorganic glasses that contain one or more of the chalcogen elements: sulfur, selenium, or tellurium covalently bonded with network formers such as Ge, As, Sb, etc. Due to the high atomic mass of the constituent elements, these glasses have low phonon energies, and thus their optical transmission range extends well into the infrared. This makes them good candidates for applications including thermal and medical imaging, biosensing, and telecommunications.[1] ChGs are also emerging as excellent materials to fabricate nonlinear optical (NLO) devices required for all-optical signal processing, because they offer an ultrafast broadband NLO response; high third order optical nonlinearity (two to three order of magnitude greater than that of silica), and low linear and nonlinear losses at telecommunications wavelengths.[2] Arsenic trisulphide (As_2S_3), one of the most widely studied of the ChGs, has been used for all-optical devices in various forms – bulk glass, optical fiber, and recently planar waveguides. Our research group (CUDOS) has reported the fabrication of As_2S_3 planar waveguides using thin film deposition and plasma etching,[3–7] and has achieved high performance NLO devices using those waveguides.[8–15]

For NLO devices the propagation loss of the waveguide is a significant factor determining performance. In general these devices exploit the high nonlinear response of a chalcogenide waveguide via processes such as self phase modulation,[11] cross phase modulation,[10,13] and four wave mixing.[12] In each case the strength of the nonlinear response is proportional to the product of the launch power, the nonlinear parameter, γ, ($\gamma=2\pi n_2/\lambda A_{eff}$), and the effective waveguide length, $L_{eff}=[1-\exp(-\alpha L)]/\alpha$ where α is the loss coefficient of the structure. Since the effective length (L_{eff}) drops with increasing propagation loss (α), loss ultimately determines the performance of the nonlinear waveguide.

The minimum attenuation possible is limited by absorption and scattering from the constituent medium. Intrinsic absorption of high purity As_2S_3 bulk glass produced by melt-quenching is known to be much less than 0.01 dB/cm in the telecommunications C-band.[16] However, the thin films which are required for the fabrication of waveguides are produced in highly nonequilibrium condition and can contain impurities, wrong bonds, structural defects, etc, which result in much higher extrinsic absorption.

So far we have concentrated on optimizing the waveguide fabrication process in order to minimize the contribution of scattering to the device losses. There are two principal scattering mechanisms; surface scattering arising from the interface between waveguide core and cladding and Rayleigh scattering from microscopic refractive index fluctuations in the material itself. Surface scattering gets stronger with increasing refractive index contrast and with the roughness of the interfaces created during the waveguide fabrication process. Generally the etched waveguide sidewalls are much rougher than the unetched top and bottom surfaces of the core so many strategies have been implemented to make the sidewalls as smooth as possible.[17] We have previously

[a]Author to whom correspondence should be addressed. Electronic mail: dyc111@physics.anu.edu.au. Tel.: +61-2-6125-9279. FAX: +61-2-6125-0029.

reported an optimized plasma etching process that creates smooth etched surfaces on As_2S_3 waveguides.[6]

In comparison Rayleigh (volume) scattering is a fundamental loss mechanism originating from inhomogeneities in the deposited films and, therefore, sets the ultimate limit on the waveguide loss. In our As_2S_3 rib-type waveguides more than 80% of the light is confined in the core and hence the contribution from Rayleigh scattering cannot be ignored. Moreover, as-deposited As_2S_3 films are known to consist of phases containing homopolar bonds (e.g., As_4S_4) interspersed with an orpiment-like (As_2S_3) backbone network.[18] Therefore, phase separation can enhance the volume scattering. There have been some reports in the literature, e.g., Ref. 19 of the effect of thermal treatment of as-deposited As_2S_3 films that have unequivocally concluded annealing accelerates the relaxation of a film toward its equilibrium state, and reduces phase separation. However, there have been little report on the influence of annealing on the performance of waveguide devices.

The purpose of this work was, therefore, twofold; first, to determine the effect of annealing of thermally deposited thin films by studying thermally-induced changes in the microstructure and optical properties of As_2S_3 thin films; and second, to fabricate and characterize waveguide devices made from as-deposited and annealed material to find out how the heat treatment affected the device performance, in particular, the propagation loss. We found that thermal annealing improves the homogeneity of as-deposited film and reduces phase separation. Consequently it reduces the propagation loss of As_2S_3 waveguides.

II. EXPERIMENTAL

As_2S_3 films either 0.85 or 2.5 μm thick were deposited by thermal evaporation onto oxidized silicon wafers in a chamber evacuated to 2×10^{-7} torr. Deposition occurred with a source to substrate distance of ~40 cm at a rate of ~0.2–0.3 nm/s. The substrates were placed in a carousel and rotated in planetary motion above the source. Prior to deposition the substrates were irradiated by a 50 eV, Ar+ beam from an ion gun for 3 min to improve adhesion of the film to the substrate. A complete description of our procedure for thermal evaporation of As_2S_3 films can be found elsewhere.[20] Some films were thermally annealed at temperatures up to but below their glass transition temperature ($T_g \approx 180$ °C) for 24 h in a vacuum oven. The refractive index and thickness of films were measured by a spectroscopic reflectometer (SCI Filmtek 4000). The surface morphology of the as-deposited and annealed films was investigated by atomic force microscopy (AFM) (Multimode SPM from Digital Instruments with Nanoscope IIIa Controller). Measurements were made using the "tapping" mode with a micromachined silicon tip (tip radius below 10 nm). The lateral step was 2 nm over a 1×1 μm^2 scan area with height resolution below 0.1 nm. The amorphicity of the films was checked by x-ray diffraction (XRD) using a PANanalytical X'Pert PRO MRD system in a glancing angle 2θ-scan. X-ray photoelectron spectroscopy (XPS) was used to study the chemical bonding of arsenic and sulfur atoms in the As_2S_3 film surface. Samples were analyzed using an EscaLab 220-IXL under a vacuum of $\sim10^{-10}$ torr. A monochromatic Al Kα x-ray source ($h\nu=1486.6$ eV) with power of 250 Watts was used for the analysis. C–C bonding was selected as the internal reference and the binding energy of C 1*s* line was referenced as 285.0 eV.

As described in our previous publications,[3,4] photolithography on As_2S_3 films is not straightforward due to attack of the films by alkaline developer solutions. Therefore, we coated the film with a thin protective layer (e.g., a bottom antireflective coating[7]) for photoresist processing. In this study a ~250 nm thick SU-8 (MicroChem) was employed for that purpose. SU-8 is ultraviolet (UV) curable, and therefore, thermal processing, which might induce a change in structural and optical properties of the film, was avoided during waveguide fabrication. Photoresist patterns were produced on the SU-8/As_2S_3 film using a Karl Suss MA6 i-line ($\lambda=365$ nm) mask aligner followed by wet development. The SU-8 and As_2S_3 layers were etched in an inductively coupled plasma reactive ion etcher (Plasmalab System 100, Oxford Instruments) utilizing oxygen-based and CHF_3 plasma, respectively. A 15 μm thick layer of inorganic polymer glass (RPO Pty Ltd, IPG™) was spin coated on top of the As_2S_3 waveguides and cured with UV light to create a top cladding. Waveguide end facets were obtained by hand cleaving the wafer along the {110} silicon cleavage planes.

The propagation loss of the guides was determined via the standard cutback method. A tunable laser source (JDS Uniphase SWS16101, 1510–1650 nm), a polarization controller, and an InGaAs power meter were used to measure the insertion loss of waveguides. Due to the small waveguide cross sectional lensed fibers which produced a mode-field diameter of ≈2.5 μm were used to couple laser light into and out of the waveguides. An Oriel mercury-xenon lamp was used as a white light source to obtain transmission spectra from the waveguide over a broad wavelength range with the aid of an Agilent 86142B optical spectrum analyzer.

III. RESULTS AND DISCUSSION

A. Thermally-induced structural and optical properties changes

The first and essential step in ChG device fabrication is to prepare high quality optical thin films with stable physical properties. It is well known that the structure and properties of ChG films are sensitive to the deposition method, and can be quite different to that of the bulk glass. This comes from the fact that films are produced in nonequilibrium conditions by rapidly condensing a vapor onto a cold substrate while the bulk glasses are produced in near equilibrium conditions by melt-quenching. As a result thermally-evaporated As_2S_3 films contain significant chemical and structural disorder such as As–As and S–S homopolar bonds which are rarely present in stoichiometric bulk glasses. In the case of As_2S_3, this results in lower density and correspondingly lower refractive index compared with the bulk.

A serious problem then arises because the physical properties of As_2S_3 films are unstable because their bond structure corresponds to a higher potential energy than that of the

ideal glass.[1] Hence the chemical bonds have a tendency to relax when the film is exposed to energy in the form of heat, light, electrons, etc. This results in a change in macroscopic properties such as the optical band gap and index of refraction with time compromising the long term stability of fabricated devices.

Thermal annealing is a simple way to accelerate the relaxation of a film into its equilibrium state since at room temperature relaxation times are of the order of a year.[21] During heat treatment it has been reported that polymerization of the structure occurs through switching of the homopolar to heteropolar bonds. Without heat treatment, As–As or S–S containing phases dispersed in the backbone network can cause enhanced Rayleigh scattering as well as elevated levels of absorption associated with exponential absorption tails extending from the band edge. Annealing also allows the film to have consistent optical properties (refractive index, optical band gap, absorption, etc) and thus improves device stability. Improved resistance to photooxidation ($As_2S_3+O_2 \rightarrow As_2O_3+S_2$) of the film is another benefit of thermal treatment.[22] These factors justify heat treatment of As_2S_3 films prior to device fabrication; however, there is very little information in the literature on the optimal annealing conditions for films used to fabricate planar waveguides and its effect on the device performance.

When heat treatment is applied to as-deposited As_2S_3 films, several requirements have to be met. First, the heat treatment should reduce inhomogeneities (phase separation, voids, dangling bonds, etc.) in the film, which are the sources of absorption and volume scattering. However, the formation of crystallites, e.g., orpiment (As_2S_3) or realgar (As_4S_4), should at the same time be avoided since these would again increase volume scattering. Second, it is important that the film surface does not roughen as a result of annealing because it forms the interface between the waveguide core and cladding and any roughening would increase surface scattering losses.[17] Finally, the significant thermal mismatch between As_2S_3 and silicon results in tensile stress in the film as a result of the heating and cooling cycle. Excessive stress can result in cracking of the film and thereby ultimately limit the maximum annealing temperature. In this work the variation of refractive index, thickness, surface roughness, and the degree of phase separation of the films were determined as a function of annealing temperatures. Based on these data we could identify the optimal annealing conditions satisfying the above requirements.

Figure 1 shows the variation in refractive index and the fractional changes in thickness and index for films annealed at temperature up to ≈170 °C. The refractive index of as-deposited films is quite low (~2.30) compared to that of the bulk glass (~2.44),[16] but increases with annealing approaching that of the bulk glass when the film was annealed close to T_g. The film thickness showed the opposite trend: decreasing with annealing temperature. Film densification ($-\Delta d/d$) contributes to the refractive index rise ($\Delta n/n$) which can be estimated through the Lorentz–Lorenz equation;

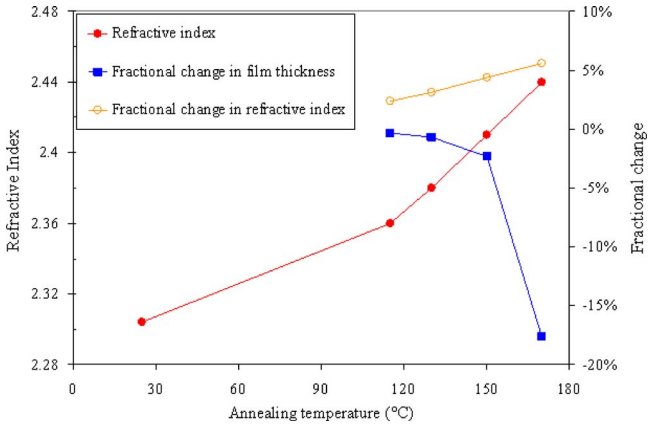

FIG. 1. (Color online) The variation in refractive index and relative thickness change in films annealed at different temperatures.

$$\frac{\Delta n}{n} = -\frac{6n^2}{(n^2-1)(n^2+2)}\frac{\Delta d}{d} \tag{1}$$

However, the relative changes in the thickness after annealing at and below 150 °C do not completely account for the observed increase in n. The extra rise in refractive index can be understood in terms of an annealing-induced increase in the number of heteropolar bonds, which form at the expense of homopolar bonds, giving rise to an increase in the effective polarizability of the material.[23] Note that the film thickness dropped sharply (~17%) above 170 °C, although the refractive index of the film continued to evolve gradually toward that of bulk. This abrupt thinning seems likely to be associated with evaporation of material from the surface at these high temperatures, which is also reflected by a sharp increase in surface roughness, as demonstrated below.

The root-mean-square (rms) roughness (R_{rms}) of the film surface was measured by AFM and is plotted against the annealing temperature in Fig. 2. R_{rms} was ~0.3 nm for as-deposited films, and remained constant as the films were annealed up to 130 °C. However, the roughness started to increase at 150 °C and became 10 times that of as-deposited film at 170 °C. As mentioned above this sharp rise in the R_{rms} is likely to be associated with evaporation of the film at high temperatures. Considering that the surface scattering

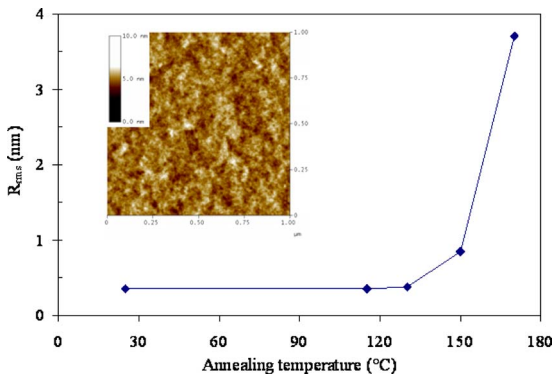

FIG. 2. (Color online) The rms roughness of the film surfaces measured by AFM and plotted against annealing temperature. The inset displays an AFM image of the As_2S_3 film (1×1 μm^2 scan area) annealed at 130 °C.

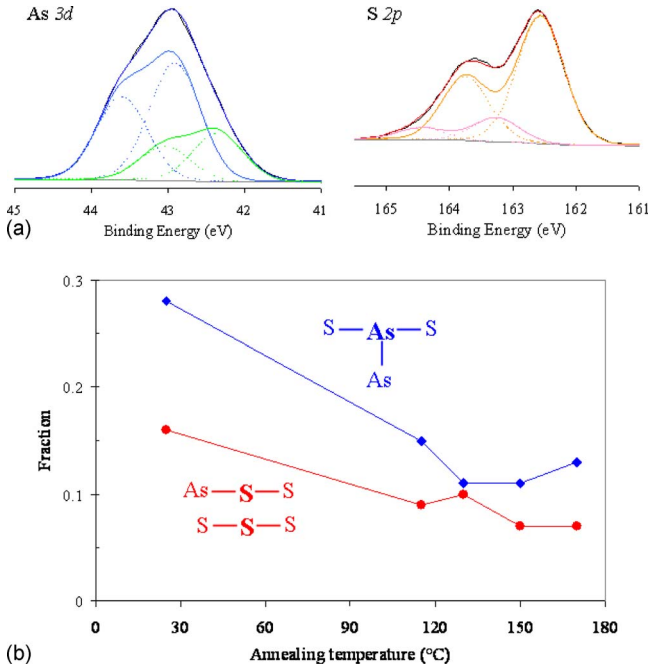

FIG. 3. (Color online) (a) The principle of obtaining the homopolar bond concentration from As 3*d* and S 2*p* spectra. As 3*d* spectrum can be decomposed into two subpeaks, blue and green lines, which correspond to arsenic atom bonded to three sulfurs and to two sulfurs and one arsenic, respectively. Each subpeak is the sum of two doublets (dashed lines). The same procedure is applied to S 2*p* spectrum. (b) The fraction of arsenic (diamonds) and sulfur (circles) atoms containing homopolar bonds in the film.

loss in a waveguide device is proportional to the R_{rms},[2] these data place an upper limit on the annealing temperature of <150 °C.

Raman scattering is a useful tool for exploring the microstructure of As_2S_3 films and bulk glasses; however, it is difficult to extract quantitative information on phase separation from Raman data. Consequently, we employed XPS to measure the concentrations of As–As and S–S homopolar bonds in the films as a function of annealing conditions. Figure 3(a) shows the principle used to obtain the homopolar bond concentration from As 3*d* and S 2*p* subshell spectra. The As 3*d* spectrum could be deconvolved into two doublets; one coming from arsenic atoms bonded to three sulfurs positioned at higher binding energy, the other from arsenic bonded to two sulfurs and one arsenic (i.e., containing an As–As homopolar bond). The details of the curve fitting procedure are given in Ref. 24. The relative fraction of As–As and S–S homopolar bond containing phases in the film is shown in Fig. 3(b) as a function of annealing temperature. It is clear that thermal treatment causes the fraction of homopolar bonds in the film to drop. However, while the refractive index of the film reached that of bulk glass, the homopolar bonds could not be completely eliminated even when the film was annealed close to T_g.

XRD was used to investigate the amorphicity of as-deposited and heat treated films (Fig. 4). To obtain usable signal intensity from these thin (≈micrometer) films we exploited the glancing incidence geometry (incident angle ≈2°–3°). Two broad peaks around 16° and 30° were observed from the as-deposited film, which is the characteristic

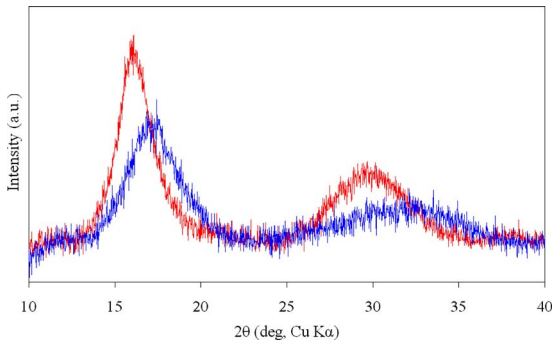

FIG. 4. (Color online) XRD patterns from as-deposited (lighter line) and heat treated (darker line) films. The glancing incidence angle was fixed at 2°–3° to get high intensity signal from the thin film. No crystal peak was detected.

of thermally evaporated As_2S_3. Upon annealing the peaks not only shifted to higher angles but also their intensities reduced. This implies that the films became denser as a result of annealing and their microstructure moved closer to that of a random glass network. No crystalline peaks could be found in the films either before of after annealing.

From these data we deduce that annealing at high temperatures is beneficial in terms of reducing phase separation and should, therefore, lead to a corresponding reduction in volume scattering. We could anticipate that light absorption would also be reduced since the existence of large numbers of homopolar bonds in the as-deposited films would lead to a defect-induced absorption tail beyond the band edge. However, taking the AFM and film thickness results into account, it is clear that the maximum annealing temperature must be kept below 150 °C to avoid an increase in the surface roughness. One more thing to note is the cracking behavior of the film. Whereas no cracks were found in thin films (below one micrometer), 2.5 μm thick films cracked at 150 °C. In further work, therefore, we limited the annealing temperature to 130 °C.

B. Optical performance: propagation losses and white light spectra

We fabricated two sets of rib-type waveguides from 0.85 and 2.5 μm thick As_2S_3 films; one set from as-deposited materials, the other from films annealed at 130 °C. The width of waveguides was 4 μm and their length up to 21 cm. Figure 5 plots the insertion loss as a function of length for waveguides obtained from 0.85 μm thick films. From the least-squares fit, we could estimate the propagation loss and coupling loss to the waveguides. The intercept to the insertion loss-axis (~6 dB) agreed well with the calculated coupling loss between the waveguide mode and a lensed fiber with mode field diameter of 2.5 μm. The propagation losses were 0.4 and 0.2 dB/cm for waveguides fabricated from as-deposited and annealed films, respectively. Similarly waveguides fabricated from 2.5 μm thick films showed losses of 0.3 and 0.05 dB/cm for as-deposited and annealed films. Thus, we found that thermal annealing reduced the propagation loss of the waveguides by 0.2–0.25 dB/cm.

These data alone do not identify the source of the additional loss present in the as-deposited films – is it due to

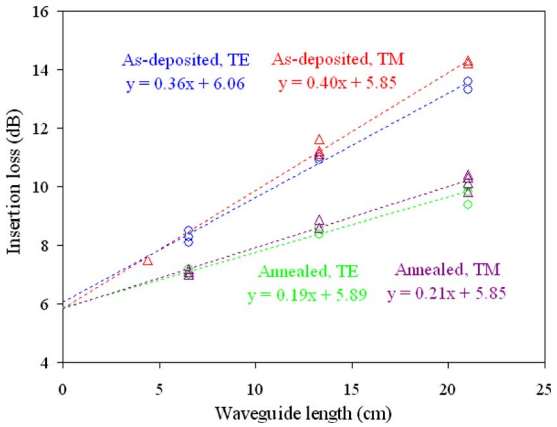

FIG. 5. (Color online) The insertion losses (in dB) of the waveguides produced from as-deposited and annealed films as a function of waveguide length. The width of the waveguides was 4 μm. The measurement was done in transverse electric and transverse magnetic polarizations and a linear equation of each case was obtained from the least square fitting method.

absorption or scattering? To elucidate its origin, we performed some additional experiments. First, we checked the roughness of the plasma-etched surfaces obtained using both as-deposited and annealed films. In a rib-type waveguide the etched sidewall is generally much rougher than unetched film interface, and thus its contribution to the scattering loss in the device is more significant. The sidewall roughness, which is difficult to measure directly, originates from lithography and the plasma etching process. Because the same lithographic process was applied to both films we presumed any lithographically induced roughness would be the same and, hence, we concentrated on the roughness of the flat etched surface to see if there was any change as a result of annealing. We found that the etched surfaces of as-deposited and thermally-annealed films had almost the same R_{rms} values (1.5 nm versus 1.6 nm) and, therefore, concluded that any loss from surface scattering was unchanged by annealing.

We then compared the white light transmission spectra for 6.5 cm long waveguides fabricated from as-deposited and annealed films and these are shown in Fig. 6. The guides have ~1.3 dB deep dips around 1.4 μm, due to the absorption from the IPG cladding.[25] Note that the insertion losses of both waveguides increases rapidly at short wavelengths, but the loss of the waveguide from the as-deposited film rises more sharply. This behavior is consistent with enhanced Rayleigh scattering which scales as λ^{-4}, and would correlate with the presence of a higher density of scatterers in the as-deposited films. Figure 3 clearly suggests that the degree of nanoscale phase separation, deduced from the homopolar bonds density was, in fact, reduced by annealing. Nevertheless, the differences between the white light transmission spectra cannot be explained assuming they are due to volume scattering alone. For instance, by comparing the spectra at short and long wavelengths, only ~25% of the difference at 1550 nm could attributed to Rayleigh scattering. This implies, therefore, that the loss due to absorption has also dropped as a result of annealing. In amorphous semiconductors such as As_2S_3 absorption at wavelengths much longer than the band edge is dominated by tail states in the band gap associated with structural disorder and network defects rather than the localized states which define the band gap itself.[26,27] A reduction in the density of homopolar bonds, defects (e.g., As_4S_4), voids, and dangling bonds by annealing would, therefore, be expected to decrease absorption in a manner consistent with our data in spite of the fact that the band gap is simultaneously red-shifted by annealing.[19] We note that our studies on non-stoichiometric glasses in the Ge–As–Se system showed a strong correlation between optical losses and the numbers of defect bonds.[28]

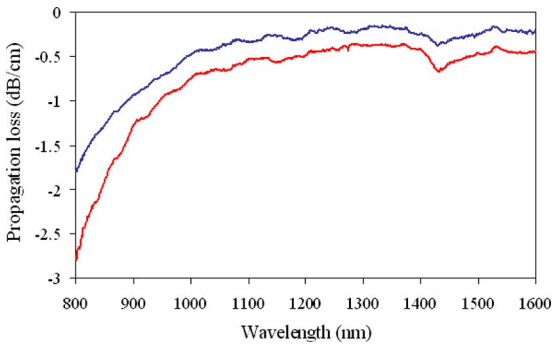

FIG. 6. (Color online) White light transmission spectra from the waveguides produced from as-deposited (lighter curve) and annealed (darker curve) films.

IV. CONCLUSION

In this work we investigated the structural and optical properties of as-deposited and thermally-annealed As_2S_3 films. The film thickness and refractive index, surface roughness, homopolar bonds content, and crystallinity were probed as a function of annealing temperature. Based on the resulting data, we identified the best annealing condition for the films (~130 °C for 24 h in a vacuum oven) that leads to the lowest loss waveguides. Characterization of waveguides produced from as-deposited and annealed films demonstrated the beneficial effect of annealing on device loss. Thermal annealing decreased the propagation loss of the waveguide by ~0.2 dB/cm. We deduced that both the Rayleigh scattering and absorption from the homopolar bonds and associated phases, voids, and dangling bonds were higher in the as-deposited films.

ACKNOWLEDGMENTS

This research was supported by the Australian Research Council through its Centre of Excellence program.

[1] P. Lucas, J. Phys.: Condens. Matter **18**, 5629 (2006).
[2] R. G. DeCorby, N. Ponnampalam, M. M. Pai, H. T. Nguyen, P. K. Dwivedi, T. J. Clement, C. J. Haugen, J. N. McMullin, and S. O. Kasap, IEEE J. Sel. Top. Quantum Electron. **11**, 539 (2005).
[3] Y. Ruan, W. Li, R. Jarvis, N. Madsen, A. Rode, and B. Luther-Davies, Opt. Express **12**, 5140 (2004).
[4] W. Li, Y. Ruan, B. Luther-Davies, A. Rode, and R. Boswell, J. Vac. Sci. Technol. A **23**, 1626 (2005).
[5] D.-Y. Choi, S. Madden, A. Rode, R. Wang, and B. Luther-Davies, J. Non-Cryst. Solids **354**, 3179 (2008).
[6] D.-Y. Choi, S. Madden, A. Rode, R. Wang, and B. Luther-Davies, J. Appl. Phys. **104**, 113305 (2008).
[7] S. Madden, D.-Y. Choi, D. Bulla, A. Rode, B. Luther-Davies, V. G. Ta'eed, M. D. Pelusi, and B. J. Eggleton, Opt. Express **15**, 14414 (2007).

[8]K. Finsterbusch, N. Baker, V. G. Ta'eed, B. J. Eggleton, D. Choi, S. Madden, and B. Luther-Davis, Electron. Lett. **42**, 1094 (2006).
[9]N. J. Baker, H. W. Lee, I. C. Littler, C. M. de Sterke, B. J. Eggleton, D.-Y. Choi, S. Madden, and B. Luther-Davies, Opt. Express **14**, 9451 (2006).
[10]V. G. Ta'eed, M. R. E. Lamont, D. J. Moss, B. J. Eggleton, D.-Y. Choi, S. Madden, and B. Luther-Davies, Opt. Express **14**, 11242 (2006).
[11]V. G. Ta'eed, N. Baker, L. Fu, K. Finsterbusch, M. R. E. Lamont, D. J. Moss, H. C. Nguyen, B. J. Eggleton, D.-Y. Choi, S. Madden, and B. Luther-Davies, Opt. Express **15**, 9205 (2007).
[12]M. D. Pelusi, V. G. Ta'eed, M. R. E. Lamont, S. Madden, D. Y. Choi, B. Luther-Davies, and B. J. Eggleton, IEEE Photon. Technol. Lett. **19**, 1496 (2007).
[13]M. R. E. Lamont, V. G. Ta'eed, M. A. F. Roelens, D. J. Moss, B. J. Eggleton, D.-Y. Choi, S. Madden, and B. Luther-Davies, Electron. Lett. **43**, 945 (2007).
[14]G. Vahid Ta'eed, Mark D. Pelusi, Benjamin J. Eggleton, Duk-Yong Choi, Steve Madden, Douglas Bulla, and Barry Luther-Davies, Opt. Express **15**, 15047 (2007).
[15]M. D. Pelusi, V. G. Ta'eed, L. B. Fu, E. Mägi, M. R. E. Lamont, S. Madden, D.-Y. Choi, D. A. P. Bulla, B. Luther-Davies, and B. J. Eggleton, IEEE J. Sel. Top. Quantum Electron. **14**, 529 (2008).
[16]http://www.amorphousmaterials.com/As-S.htm
[17]F. Grillot, L. Vivien, S. Laval, D. Pascal, and E. Cassan, IEEE Photon. Technol. Lett. **16**, 1661 (2004).
[18]D. G. Georgiev, P. Boolchand, and K. A. Jackson, Philos. Mag. **83**, 2941 (2003).
[19]J. P. De Neufville, S. C. Moss, and S. R. Ovshinsky, J. Non-Cryst. Solids **13**, 191 (1974).
[20]D. A. P. Bulla, R. P. Wang, A. Prasad, A. V. Rode, S. J. Madden, and B. Luther-Davies, Appl. Phys. A: Mater. Sci. Process. **96**, 615 (2009).
[21]A. V. Kolobov and G. J. Adriaenssens, Philos. Mag. B **69**, 21 (1994).
[22]J.-F. Viens, C. Meneghini, A. Villeneuve, T. V. Galstian, E. J. Knystautas, M. A. Duguay, K. A. Richardson, and T. Cardinal, J. Lightwave Technol. **17**, 1184 (1999).
[23]E. Márquez, J. M. González-Leal, R. Jiménez-Garay, and M. Vlcek, Thin Solid Films **396**, 184 (2001).
[24]D.-Y. Choi, S. Madden, A. Rode, R. Wang, and B. Luther-Davies, J. Appl. Phys. **102**, 083532 (2007).
[25]S. J. Madden, M. Y. Zhang, D.-Y. Choi, B. Luther-Davies, and R. Charters, J. Vac. Sci. Technol. A **27**, 561 (2009).
[26]R. A. Street, R. J. Nemanich, and G. A. N. Connell, Phys. Rev. B **18**, 6915 (1978).
[27]D. L. Wood and J. Tauc, Phys. Rev. B **5**, 3144 (1972).
[28]A. Prasad, C.-J. Zha, R.-P. Wang, A. Smith, S. Madden, B. Luther-Davies, Opt. Express **16**, 2804 (2008).